



INVESTIGATION OF NOISE IN SURFACE TOPOGRAPHY MEASUREMENT USING STRUCTURED ILLUMINATION MICROSCOPY

Zhen Li, Sophie Gröger

Chemnitz University of Technology, Department of Production Measuring Technology, Reichenhainer Straße 70, 09126 Chemnitz, Germany (✉ zhen.li@s2018.tu-chemnitz.de, +49 371 531 981 250, sophie.groeger@mb.tu-chemnitz.de)

Abstract

Noise is a fundamental metrological characteristic of the instrument in surface topography measurement. Therefore, measurement noise should be thoroughly studied in practical measurement to understand instrument performance and optimize measurement strategy. This paper investigates the measurement noise at different measurement settings using structured illumination microscopy. The investigation shows that the measurement noise may scatter significantly among different measurement settings. Eliminating sample tilt, selecting low vertical scanning interval and high exposure time is helpful to reduce the measurement noise. In order to estimate the influence of noise on the measurement, an approach based on metrological characteristics is proposed. The paper provides a practical guide to understanding measurement noise in a wide range of applications.

Keywords: surface topography measurement, measurement noise, uncertainty, structured illumination microscopy.

© 2021 Polish Academy of Sciences. All rights reserved

1. Introduction

Noise is one of vital metrological characteristics of areal topography measuring methods. The terminology of noise, including instrument noise, measurement noise, static noise, and dynamic noise, is defined in ISO 25178-600 [1]. Instrument noise is the internal noise caused by the instrument if ideally placed in a noise-free environment. However, measurement noise occurs during realistic measurement, where there are many other influential factors. Consequently, measurement noise is usually higher than instrument noise. In other words, instrument noise can be considered the minimum achievable value for measurement noise [2]. In addition, measurement noise may scatter significantly in different instruments [3, 4].

There are various noise sources in surface topography measurement, *e.g.*, noise caused by instrument electronics, external electromagnetic disturbances, and vibrations [5], noise due to temperature fluctuations [6], scattering noise and background noise [7]. Sample placement is

another factor because there are more vibration and air turbulence effects at a tilted sample than when the tilt is eliminated [8,9]. Noise is of great importance in surface topography measurement. Measurement noise limits instrument capability of measuring high spatial frequencies [10]. Furthermore, measurement noise can limit measurement repeatability as well [11, 12]. Due to noise bias [13], there can also be a systematic deviation in the height parameter, which is not revealed by repeated measurements [14].

Subtraction method [15, 16] and averaging method [13] are common methods to determine measurement noise in surface topography measurement [5]. A smooth flat surface such as an optical mirror is widely used as the material measure. For the subtraction method, two consecutive measurements should be carried out at the same sample position in a short time. For the averaging method, several repeated measurements are carried out in a short time. The subtraction method and averaging method are equivalent when the number of repeated measurements is two. Furthermore, noise density is defined to describe the relationship between the measurement noise, data acquisition time and array size [2, 17]. It is worth noting that the existence of non-measured points is a problem using optical methods [18]. The handling of the non-measured points affects the estimation of measurement noise and should be reported.

Filtering is commonly used to suppress the measurement noise [19, 20]. Various filters can suppress the noise, such as the Gaussian filter, robust Gaussian filter, median filter, spline filter, morphological filter, and wavelets filter. The comparisons between different filters were made elsewhere [21–25]. In addition, the Fourier decomposition approach [13] and the Legendre polynomial decomposition approach [26] have been proved to reduce the noise apart from conventional filtering. Moreover, optimizing the measurement process is another option to reduce the noise. For example, it could be topography averaging and signal oversampling [27], optimizing object placement [28], and minimizing the environmental temperature fluctuations [11].

In order to optimize the measurement strategy, understanding measurement noise and estimating its influence on measurement is meaningful in practical measurement. In addition to the noise reduction method mentioned above, the operator can also consider reducing the noise in the measurement data acquisition by selecting proper measurement settings. Therefore, this paper studies the measurement noise in practical measurement using *structured illumination microscopy* (SIM). The aims of the study are: (1) to investigate the influence of lens, vertical scanning interval (sampling distance in the depth direction), exposure time, and sample tilt on the measurement noise, and (2) to estimate the influence of noise on the measurement result.

2. Material and methods

2.1. Instrumentation

The measurements were performed using a confovis Duo Vario measuring system with structured illumination. The measurement principle of structured illumination is shown as in [29]:

As can be seen in Fig. 1, LED A and LED B are actuated alternately during the measurement. The grid pattern is projected on the measured topography by transmission when LED A is activated. The grid pattern is projected on the measured topography by reflection when LED B is activated. Therefore, the image sensor captures the surface with the imaged grid, generating two 180° phase-shifted images during the measurement. If the measured topography is in focus, the grid pattern is sharply imaged. As a result, the contrast difference (C) between individual images is high. When the measured topography is out of the focal plane, the contrast difference (C) is low. Consequently, the height of the surface is determined by the contrast difference (C). The selected instrument parameters and corresponding values are shown in Table 1.

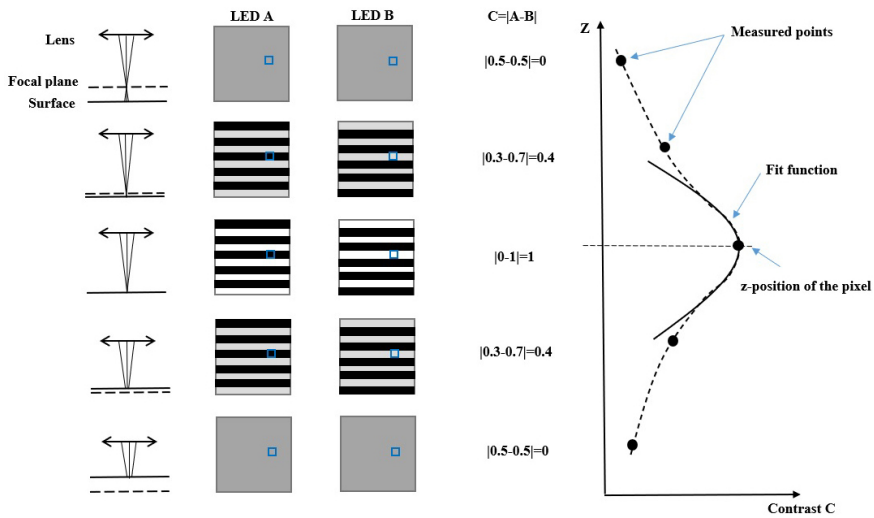


Fig. 1. Schematic diagram of the structured illumination method [29].

Table 1. Selected process parameters and their values in the measurement system.

Lens	NA	Acceptance angle / °	FoV / (µm × µm)	Lateral sampling interval/ µm
20 × magnification	0.60	36.9	630 × 630	0.248
50 × magnification	0.95	71.8	254 × 254	0.099

2.2. Samples

In this work, a silver-plated mirror surface and three grinding surfaces were measured. Fig. 2 shows a pseudo-color view of the samples' surfaces. Five repeated measurements were carried out with a 20 × lens at 0.05 µm vertical scanning interval to obtain information for each surface. This information was obtained according to the ISO 25178-2 standard [30]. *Sq* (root mean square height of the scale-limited surface) was used to indicate roughness. *Sdq* (root mean square gradient of the scale-limited surface) was used to indicate surface complexity.

For parameter calculation, outliers were removed, non-measured points were filled and the surface was levelled by subtracting the least-squares plane. Because the lateral sampling interval was 0.248 µm, an S-filter with a nesting index of 0.8 µm was applied according to ISO 25178-3 [19]. Moreover, an L-filter with a nesting index of 250 µm was applied at a 300:1 bandwidth ratio. Table 2 shows mean values of *Sq* and *Sdq* from five repeated measurements.

Table 2. Samples and mean values of areal surface texture parameters.

Samples	Symbols	<i>Sq</i>	<i>Sdq</i>
Silver-plated mirror surface	SS	3.1 nm	0.008
grinding surface 1	GS_1	0.19 µm	0.14
grinding surface 2	GS_2	0.45 µm	0.27
grinding surface 3	GS_3	0.83 µm	0.29

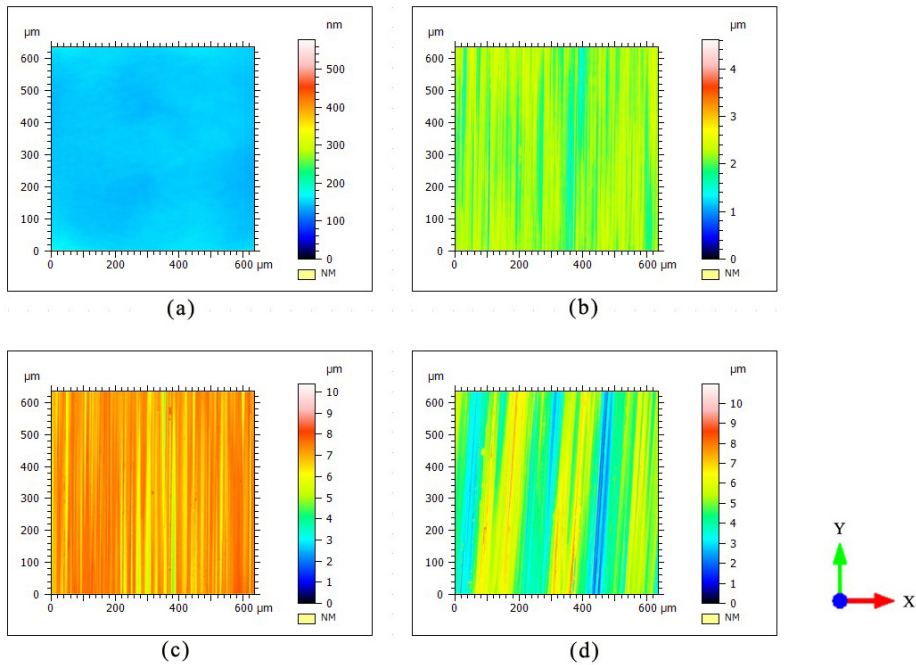


Fig. 2. Pseudo-color view of the measured surfaces. SS (a), GS_1 (b), GS_2 (c), and GS_3 (d).

2.3. Assessment of the measurement noise

The measurement noise may significantly scatter at some measurement settings. Therefore, stabilized measurement noise was estimated in this work. There were five surface topographies (M1, M2, M3, M4, and M5) from five repeated measurements. Four noise topographies (M1-M2, M2-M3, M3-M4, M4-M5) were generated by surface subtraction. First, the measurement noise from four noise topographies was established by (1). Then according to ISO/DIS 25178-700 [31], the stabilized measurement noise was estimated by (2).

$$N_M = \frac{Sq_{\text{difference}}}{\sqrt{2}}, \quad (1)$$

where N_M is measurement noise and $Sq_{\text{difference}}$ is the root mean square height of the noise topography.

$$\bar{N}_M = \sqrt{\frac{1}{P} \sum_{i=1}^P N_{MP}^2}, \quad (2)$$

where \bar{N}_M is the stabilized measurement noise and N_{MP} is the P -th assessment of the measurement noise according to (1).

In practical measurement, the non-measured points can be filled by interpolation or just omitted. The estimation of measurement noise should correspond to post-processing of the measurement data. In this work, the non-measured points were filled before calculating areal surface texture parameters. Therefore, the non-measured points were analogously filled before surface subtraction.

2.4. Assessment of uncertainty due to measurement noise

The uncertainty component includes noise bias on parameter calculation and measurement repeatability caused by noise [14]. Therefore, the combined uncertainty due to noise can be written as

$$u_{S\text{-noise}}^2 = u_{S\text{-repeat}}^2 + u_{S\text{-bias}}^2, \quad (3)$$

where $u_{S\text{-noise}}$ is the combined uncertainty of parameter S due to noise, $u_{S\text{-bias}}$ is the uncertainty of parameter S due to noise bias, and $u_{S\text{-repeat}}$ is the uncertainty of parameter S due to repeatability caused by noise.

The standard deviation of repeated measurements represents the uncertainty due to repeatability. As an illustration, Fig. 3 shows the approach to assess the uncertainty due to noise bias based on metrological characteristics [32, 33]. Noise topography was first generated by subtraction of two consecutive measured surface topographies. Then the noise topography was added to or subtracted from the original surface topography, and parameter variation (Δ_i) was estimated. The same process was performed n times in succession, and a series of parameter variations was obtained. The standard uncertainty $u(S)$ was finally estimated.

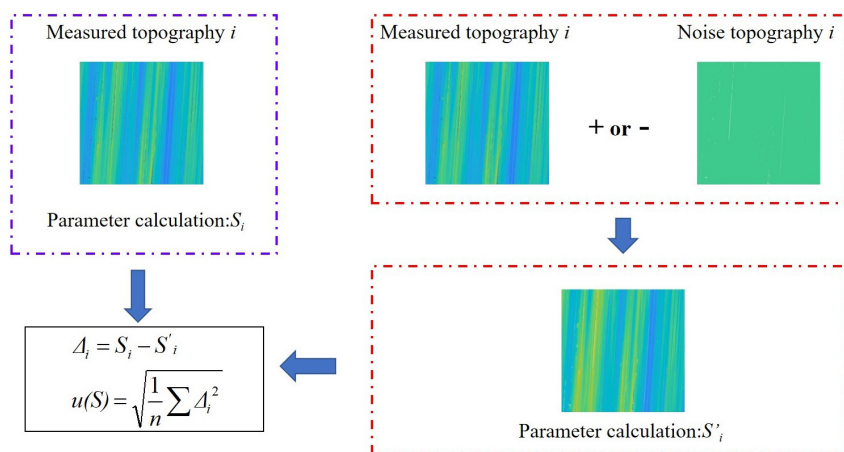


Fig. 3. The illustration of estimating uncertainty due to noise bias.

3. Results and discussion

3.1. Measurement noise at different objective lens

The measurement was carried out with 20× lens and 50× lens, respectively. When the lens was changed, the sample was not moved, and the *field of view* (FoV) centre was always at the same position on the sample surface. The largest exposure time was set in the absence of over-saturated points. Selected measurement settings are shown in Table 3; only the vertical scanning interval changed after the lens and exposure time were fixed. A 254 $\mu\text{m} \times 254 \mu\text{m}$ centre region was extracted for every measurement data with a 20× lens. Therefore, the estimation of the measurement noise was from the same region of the 20× lens and the 50× lens.

A high *numerical aperture* (NA) lens has advantages such as small width of the contrast curve shown in Fig. 1 [34], high *signal to noise ratio* (SNR) due to high light intensity, high lateral

Table 3. Selected measurement settings.

Sample	Lens	Exposure time / ms	Vertical scanning interval / μm
SS	20 \times	1.26	0.05, 0.1, 0.2
	50 \times	4.43	0.05, 0.1, 0.2
GS_1	20 \times	1.37	0.05, 0.1, 0.2
	50 \times	4.54	0.05, 0.1, 0.2
GS_2	20 \times	1.3	0.05, 0.1, 0.2
	50 \times	4.58	0.05, 0.1, 0.2
GS_3	20 \times	1.22	0.05, 0.1, 0.2
	50 \times	4.32	0.05, 0.1, 0.2

resolution, and good handling capability of the large slope because of a wide acceptance angle. Therefore, in general, the measurement noise using a 50 \times lens was lower than using a 20 \times lens regardless of measuring rough or smooth surface. The result in Fig. 4c and Fig. 4d agree with the analysis.

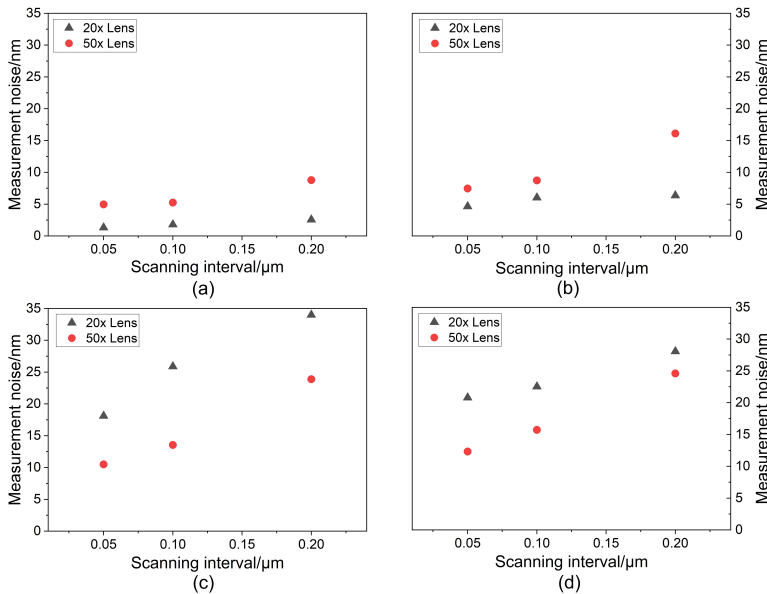


Fig. 4. Stabilized measurement noise at different lens. SS (a), GS_1 (b), GS_2 (c), and GS_3 (d).

Fig. 4a and Fig. 4b show that the stabilized measurement noise was higher with the 50 \times lens than with the 20 \times lens in the smooth surface measurement. The reason was that the environment-induced noise phenomenon was more likely to be noticed during the smooth surface measurement. There was, for example, noise caused by vibration. A high NA lens with high lateral resolution captured more noise detail. However, a low NA lens captured less noise detail due to the average effect of low resolution. Another possible reason was the accumulated background noise due to high exposure time.

3.2. Measurement noise at different vertical scanning intervals

Fig. 4 shows that the stabilized measurement noise increased with the increase of the vertical scanning interval. This was because when the vertical scanning interval increased, fewer images were captured during the scanning. As a result, the calculation accuracy of the height value based on the contrast curve fit decreased due to lower point density. According to [34], the measured height precision of the SIM follows the square root of the vertical scanning interval. Accordingly, there would be a similar relation between the measurement noise and the vertical scanning interval.

A linear regression fit was created for the measurement noise versus the square root of the vertical scanning interval, as shown in Fig. 5. The measurement noise established by (1) was used instead of the stabilized measurement noise for a reliable fit. The R-Squared value indicates that the measurement noise was linearly related to the square root of the vertical scanning interval. It is worth noting that the R-Squared value of GS_1 with the 20× lens was 0.4 but it exceeded 0.8 when the linear fit was created using the stabilized measurement noise. Sometimes, it is not possible to get the exact measurement time to estimate the noise density. However, the linear regression fit method shown in Fig. 5 could be an option.

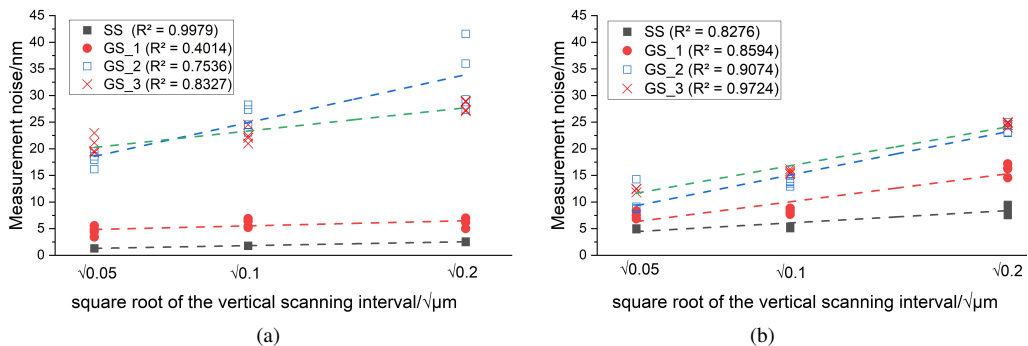


Fig. 5. Relationship of measurement noise and the square root of the vertical scanning interval. R-squared (R^2) is a goodness-of-fit measure for linear regression models. 20× lens (a) and 50× lens (b).

There is another issue that needs attention. As shown in Fig. 5, the measurement noise established by (1) was not stable for measuring rough surfaces or measurement at large vertical scanning intervals. Taking measurement noise with the 20× lens at 0.2 μm vertical scanning interval as an example, the standard deviation of the measurement noise of SS and GS_2 was 0.03 nm and 6.5 nm, respectively. Therefore, the measurement noise estimated by subtraction of the two topographies is sufficient for the smooth surface measurement. Establishing the stabilized measurement noise or establishing the measurement noise by the averaging method is suggested for rough surface measurement.

3.3. Measurement noise at different exposure times

The influence of exposure time on the measurement noise was investigated at 0.1 μm vertical scanning interval. When the lens had been selected, the measurements were carried out at five different exposure times where the values changed by almost 40% over the measurement. Measuring the SS surface with the 20× lens as an example, 1.26 ms was the maximum exposure time in the absence of over-saturated points. Therefore, the measurements were carried out at

exposure times of 1.26 ms, 1.13 ms, 1.02 ms, 0.92 ms, and 0.83 ms, respectively. Because there was no direct comparison between the 20× lens and the 50× lens, the whole FoV was used to estimate the measurement noise for every measurement.

As shown in Fig. 6, if the 50× lens was used, the stabilized measurement noise decreased when the exposure time increased. The reason was that the SNR increased as a result of increasing exposure time. It appears, however, that the variation of measurement noise was not significant with the 20× lens. The reason was that variation of exposure time did not significantly affect SNR which could be verified by the *non-measured point percentage* (NMP). In general, increasing SNR can decrease the NMP which is evident at surfaces with high roughness [35]. Taking GS_3 surface as an example, when the 20× lens was used, the average NMP of five repeated measurements was 2.3% and 2.6% at 1.2 ms and 0.8 ms, respectively; When the 50× lens was used, the average NMP was 2.6% and 6% at 4.32 ms and 2.84 ms, respectively. Thus, it indicates that the selected variation of exposure time significantly affected the measurement with the 50× lens. From the practical viewpoint, high exposure time in the absence of over-saturated points is recommended to reduce the measurement noise.

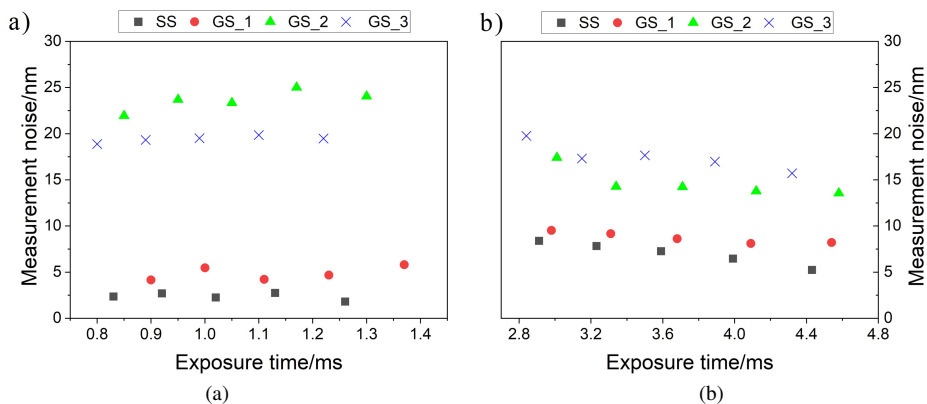


Fig. 6. Stabilized measurement noise at different exposure times. 20× lens (a) and 50× lens (b).

3.4. Tilted-sample measurement noise

The relation between the measurement noise and sample tilt was investigated with a 20× lens at a 0.1 μm vertical scanning interval. A manual goniometer stage first eliminated the sample tilt, and this position was set as the reference position. Then the sample was tilted around the X axis of the stage, in the range of $\pm 2^\circ$ with respect to the reference position. The sample was also analogously tilted around the Y axis. While tilting, it was ensured that the centre of the FoV was always at the same position on the measured surface. Five repeated measurements were carried out at each tilt angle. The maximum exposure time was selected assuming the absence of over-saturated points over the measurements.

As shown in Fig. 7, the stabilized measurement noise varied at the different tilt angles. Fig. 8a and Fig. 8b show that there were stripes on the noise topography of the SS when the sample was tilted which illustrates that there was correlated noise. It could be caused by the environment such as vibration and air turbulence [9]. However, there was no significant stripe pattern on the noise topography when the sample was at the horizontal position. It indicates that this correlated noise had more effects on the tilted sample.

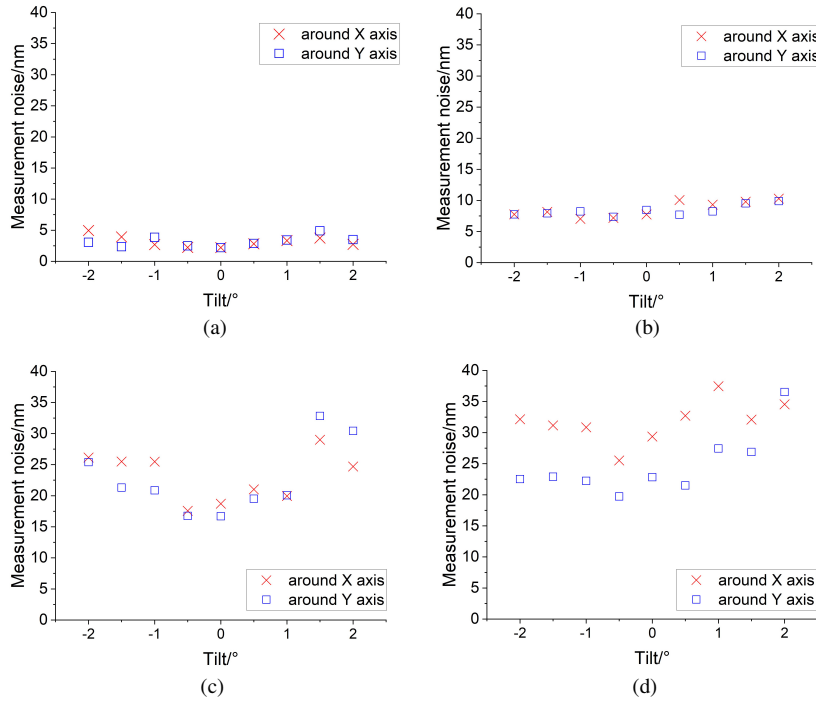


Fig. 7. Stabilized measurement noise at different tilt angles. SS (a), GS_1 (b), GS_2 (c), and GS_3 (d).

For the smooth surface, the tilt caused that some part of the light was not reflected on the lens and the SNR decreased. This was another possible factor affecting the measurement noise which would be evident at a high tilt angle. In addition, there is slope dependent error in the optical instrument [36]. How the slope dependent error of SIM affects the measurement noise needs further study.

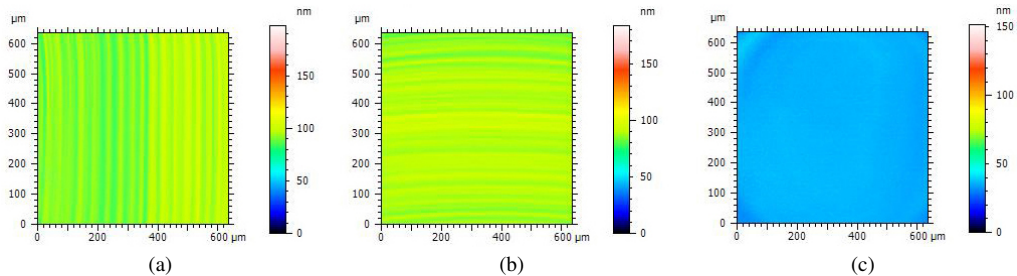


Fig. 8. Noise topographies of SS at 2° tilt around Y axis (a), at 2° tilt around X axis (b), and no tilt (c).

3.5. Measurement uncertainty due to noise

The uncertainties of ISO 25178-2 areal surface texture height parameters [30] were taken as examples in this work. The height parameters include Sq (root mean square height of the scale-limited surface), Sa (arithmetical mean height of the scale-limited surface), Ssk (skewness of the

scale-limited surface), Sku (kurtosis of the scale-limited surface), Sp (maximum peak height of the scale-limited surface), Sv (maximum pit height of the scale-limited surface), and Sz (maximum height of the scale-limited surface). The data was from five repeated measurements with the 20× lens at 0.05 μm vertical scanning intervals. The parameter calculation was performed with the same procedure as in Section 2.2.

Table 4 shows that the uncertainty of Sq and Sa due to measurement noise was low, less than 1 nm. However, contrary to this, the uncertainty of Sp , Sv , and Sz was high, even tens of nanometers. The reason is that the Sq and Sa are measures of the entire surface's height variation. Sp , Sv , and Sz are extreme height parameters.

Table 4. Measurement uncertainty due to measurement noise.

Uncertainty type	Samples	U_{Sq} / nm	U_{Ssk}	U_{Sku}	U_{Sp} / nm	U_{Sv} / nm	U_{Sz} / nm	U_{Sa} / nm
Uncertainty due to repeatability	SS	0.02	0.02	0.09	5.81	4.41	3.26	0.01
	GS_1	0.12	0.00	0.02	25.70	7.59	25.64	0.12
	GS_2	0.52	0.00	0.01	20.61	9.05	18.05	0.59
	GS_3	0.31	0.00	0.00	4.16	14.18	16.88	0.30
Uncertainty due to noise bias	SS	0.24	0.01	0.12	7.73	3.73	5.41	0.20
	GS_1	0.20	0.00	0.01	34.80	5.52	39.19	0.17
	GS_2	0.76	0.00	0.01	12.67	32.15	40.01	0.71
	GS_3	0.58	0.00	0.00	33.55	24.54	19.58	0.55
Combined uncertainty	SS	0.24	0.02	0.15	9.67	5.78	6.32	0.20
	GS_1	0.23	0.00	0.02	43.26	9.39	46.83	0.21
	GS_2	0.92	0.00	0.01	24.19	33.40	43.89	0.92
	GS_3	0.66	0.00	0.00	33.81	28.34	25.85	0.63

The height values are small on the smooth surface and as such they are easily affected by the noise. However, the height values are large on the rough surface. The noise amplitude is too low to affect the height distribution of the rough surface. This is why the uncertainty of Ssk and Sku due to measurement noise was high at the smooth surface measurement and low at the rough surface measurement.

It should be noted that the uncertainty is related to the filtering, handling of non-measured points and outliers. Consequently, the measurement uncertainty varies depending on the data processing method. The proposed approach can evaluate how the noise affects the measurement result but is limited by the number of measurements times. Increasing the repeated measurements times could improve the accuracy of the uncertainty estimation.

4. Conclusions and future work

In this work, measurement noise at different measurement settings was investigated using SIM. In addition, it was studied how the noise affected height parameters. The work provides a practical guide to understanding measurement noise in a wide range of applications.

It is shown that measurement noise scatters among different measurement settings. Therefore, measurement noise should be estimated at the settings where the instrument is applied.

Eliminating sample tilt, selecting low vertical scanning interval and high exposure time is helpful to reduce the measurement noise. In general, using a high NA lens can reduce the

measurement noise. However, if there is environment-induced noise, using a high NA lens may not reduce the measurement noise in the smooth surface measurement.

Measurement noise scatters while measuring rough surfaces or measuring at large vertical scanning intervals. In this case, establishing measurement noise by the averaging method or using stabilized measurement noise is recommended.

The metrological characteristics approach is capable estimating the uncertainty due to measurement noise. Sq and Sa are not sensitive to the noise, while Sp , Sv , and Sz are sensitive to the noise. The uncertainty of Ssk and Sku is higher in smooth surface measurement than in rough surface measurement.

More samples with different structures and materials will be measured to investigate the measurement noise in the future.

Acknowledgements

The author Zhen Li acknowledges the Chinese Scholarship Council (CSC) for funding his doctoral study.

References

- [1] International Organization for Standardization. (2019). *Geometrical product specifications (GPS) – Surface texture: Areal – Part 600: Metrological characteristics for areal topography measuring methods* (ISO 25178-600:2019). <https://www.iso.org/standard/67651.html>
- [2] de Groot, P., & DiSciaccia, J. (2020). Definition and evaluation of topography measurement noise in optical instruments. *Optical Engineering*, 59(6), 064110. <https://doi.org/10.1117/1.OE.59.6.064110>
- [3] Eifler, M., Hering, J., Seewig, J., Leach, R. K., von Freymann, G., Hu, X., & Dai, G. (2020). Comparison of material measures for areal surface topography measuring instrument calibration. *Surface Topography: Metrology and Properties*, 8(2), 025019. <https://doi.org/10.1088/2051-672X/ab92ae>
- [4] Vanrusselt, M., Haitjema, H., Leach, R., & de Groot, P. (2021). International comparison of noise in areal surface topography measurements. *Surface Topography: Metrology and Properties*, 9(2), 025015. <https://doi.org/10.1088/2051-672X/abfa29>
- [5] Giusca, C. L., Leach, R. K., Helary, F., Gutauskas, T., & Nimishakavi, L. (2012). Calibration of the scales of areal surface topography-measuring instruments: Part 1. Measurement noise and residual flatness. *Measurement Science and Technology*, 23(3), 035008. <https://doi.org/10.1088/0957-0233/23/3/035008>
- [6] Grochalski, K., Wiczorowski, M., Pawlus, P., & H'Roura, J. (2020). Thermal sources of errors in surface texture imaging. *Materials*, 13(10), 2337. <https://doi.org/10.3390/ma13102337>
- [7] Fu, S., Cheng, F., Tjahjowidodo, T., Zhou, Y., & Butler, D. (2018). A non-contact measuring system for in-situ surface characterization based on laser confocal microscopy. *Sensors*, 18(8), 2657. <https://doi.org/10.3390/s18082657>
- [8] Barker, A., Syam, W. P., & Leach, R. K. (2016, October). Measurement noise of a coherence scanning interferometer in an industrial environment. *Proceedings of the Thirty-First Annual Meeting of the American Society for Precision Engineering* (vol. 65, pp. 594–599). <http://eprints.nottingham.ac.uk/id/eprint/38454>
- [9] Gomez, C., Su, R., De Groot, P., & Leach, R. (2020). Noise reduction in coherence scanning interferometry for surface topography measurement. *Nanomanufacturing and Metrology*, 3, 68–76. <https://doi.org/10.1007/s41871-020-00057-4>

- [10] Leach, R. (Ed.). (2011). *Optical Measurement of Surface Topography* (Vol. 8). Springer Berlin Heidelberg. <https://doi.org/10.1007/978-3-642-12012-1>
- [11] Maculotti, G., Feng, X., Galetto, M., & Leach, R. (2018). Noise evaluation of a point autofocus surface topography measuring instrument. *Measurement Science and Technology*, 29(6), 065008. <https://doi.org/10.1088/1361-6501/aab528>
- [12] De Groot, P. J. (2017). The meaning and measure of vertical resolution in optical surface topography measurement. *Applied Sciences*, 7(1), 54. <https://doi.org/10.3390/app7010054>
- [13] Haitjema, H., & Morel, M. A. A. (2005). Noise bias removal in profile measurements. *Measurement*, 38(1), 21–29. <https://doi.org/10.1016/j.measurement.2005.02.002>
- [14] Leach, R., Haitjema, H., Su, R., & Thompson, A. (2020). Metrological characteristics for the calibration of surface topography measuring instruments: a review. *Measurement Science and Technology*, 32(3), 032001. <https://doi.org/10.1088/1361-6501/abb54f>
- [15] DIN. (2008). *Optical measurement and microtopographies – Calibration of interference microscopes and depth measurement standards for roughness measurement* (VDI/VDE 2655 Blatt 1.1).
- [16] DIN. (2010). *Optical measurement of microtopography – Calibration of confocal microscopes and depth setting standards for roughness measurement* (VDI/VDE 2655 Blatt 1.2).
- [17] de Groot, P., & DiSciaccia, J. (2018, August). Surface-height measurement noise in interference microscopy. *Interferometry XIX* (Vol. 10749, p. 107490Q). International Society for Optics and Photonics. <https://doi.org/10.1117/12.2323900>
- [18] Pawlus, P., Reizer, R., & Wieczorowski, M. (2017). Problem of non-measured points in surface texture measurements. *Metrology and Measurement Systems*, 24(3), 525–536. <https://doi.org/10.1515/mms-2017-0046>
- [19] International Organization for Standardization. (2012). Geometrical product specifications (GPS) – Surface texture: Areal – Part 3: Specification operators (ISO 25178-3:2012).
- [20] Blateyron, F. (2014, May). Good practices for the use of areal filters. *Proc. 3rd Seminar on Surface Metrology of the Americas*.
- [21] Podulka, P. (2020). Proposal of frequency-based decomposition approach for minimization of errors in surface texture parameter calculation. *Surface and Interface Analysis*, 52(12), 882–889. <https://doi.org/10.1002/sia.6840>
- [22] He, B., Zheng, H., Ding, S., Yang, R., & Shi, Z. (2021). A review of digital filtering in surface roughness evaluation. *Metrology and Measurement Systems*, 28(2). <https://doi.org/10.24425/mms.2021.136606>
- [23] Podulka, P. (2020). Comparisons of envelope morphological filtering methods and various regular algorithms for surface texture analysis. *Metrology and Measurement Systems*, 27(2), 243–263. <https://doi.org/10.24425/mms.2020.132772>
- [24] Podulka, P. (2021). Reduction of Influence of the High-Frequency Noise on the Results of Surface Topography Measurements. *Materials*, 14(2), 333. <https://doi.org/10.3390/ma14020333>
- [25] Todhunter, L., Leach, R., & Blateyron, F. (2020). Mathematical approach to the validation of surface texture filtration software. *Surface Topography: Metrology and Properties*, 8(4), 045017. <https://doi.org/10.1088/2051-672X/abc0fb>
- [26] Vanrusselt, M., & Haitjema, H. (2020). Reduction of noise bias in 2.5 D surface measurements. In *Proceedings of Euspen's 20th International Conference & Exhibition*, 277–281. European Society for Precision Engineering; Northampton.
- [27] Gomez, C., Su, R., Lawes, S., & Leach, R. (2019). Comparison of two noise reduction methods in coherence scanning interferometry for surface measurement. *The 14th International Symposium on Measurement Technology and Intelligent Instruments*.

- [28] Sánchez, Á. R., Thompson, A., Körner, L., Brierley, N., & Leach, R. (2020). Review of the influence of noise in X-ray computed tomography measurement uncertainty. *Precision Engineering*, 66, 382–391. <https://doi.org/10.1016/j.precisioneng.2020.08.004>
- [29] confovis GmbH. *Structured Illumination Microscopy*. <https://www.confovis.com/en/optical-measurement>
- [30] International Organization for Standardization. (2012). *Geometrical product specifications (GPS) – Surface texture: Areal – Part 2: Terms, definitions and surface texture parameters (ISO 25178-2:2012)*.
- [31] International Organization for Standardization. (2020). *Geometrical product specifications (GPS) – Surface texture: Areal – Part 700: Calibration, adjustment and verification of areal topography measuring instruments (ISO/DIS 25178-700:2020)*.
- [32] Leach, R., Haitjema, H., & Giusca, C. (2019). A metrological characteristics approach to uncertainty in surface metrology. *Optical Inspection of Microsystems*, 73–91. CRC Press.
- [33] Haitjema, H. (2015). Uncertainty in measurement of surface topography. *Surface Topography: Metrology and Properties*, 3(3), 035004. <https://doi.org/10.1088/2051-672X/3/3/035004>
- [34] Yang, Z., Kessel, A., & Häusler, G. (2015). Better 3D Inspection with Structured Illumination: Signal Formation and Precision. *Applied Optics*, 54(22), 6652–6660. <https://doi.org/10.1364/AO.54.006652>
- [35] Gomez, C., Su, R., Thompson, A., DiSciaccia, J., Lawes, S., & Leach, R. K. (2017). Optimization of surface measurement for metal additive manufacturing using coherence scanning interferometry. *Optical Engineering*, 56(11), 111714. <https://doi.org/10.1117/1.OE.56.11.111714>
- [36] Zhou, Y., Troutman, J., Evans, C., & Davies, A. (2014, June). Using the random ball test to calibrate slope dependent errors in optical profilometry. *Optical Fabrication and Testing*, OW4B-2. Optical Society of America. <https://doi.org/10.1364/OFT.2014.OW4B.2>



Zhen Li received his B.Eng. degree and M.Eng. degree from Hefei University of Technology, China, in 2006 and 2013, respectively. He is currently pursuing a Ph.D. degree at Chemnitz University of Technology, Germany. His main research interest are precision measurement technology and instruments.



Sophie Gröger received her Ph.D. degree from Chemnitz University of Technology, Germany, in 2007. She is currently Full Professor and Head of the Production Measuring Technology Department in the Chemnitz University of Technology. Her current research interests include Geometrical Product Specification and optical as well as tactile geometrical measurements. She is a member of the national and international standardization committees on Geometrical Product Specification and Verification.